

04
Pin-hole camera based soft X-ray solar telescope for nanosatellite

© S.V. Kuzin,¹ A.S. Kirichenko,^{2,3} A.A. Pertsov,^{1,3} S.A. Bogachev,^{2,3} N.F. Erkhova⁴

¹ Institute Of Solar-Terrestrial Physics Of Siberian Branch Of Russian Academy Of Sciences (ISTP SB RAS), 664033 Irkutsk, Russia

² Institute of Space Research, Russian Academy of Sciences, 117997 Moscow, Russia

³ Samara National Research University, 443086 Samara, Russia

⁴ Lebedev Physical Institute, Russian Academy of Sciences, 119991 Moscow, Russia
e-mail: kuzin@iszf.irk.ru

Received April 19, 2022

Revised April 19, 2022

Accepted April 19, 2022

Pin-hole camera as a soft X-ray solar telescope is presented. The instrument is aimed on imaging of flares in the solar corona with angular resolution up to 40". It will allow to register temporal profiles of flares and determine spectra in soft X-ray. The telescope consist on pin hole 0.1 mm in diameter in tungsten disk, thin film Al/maylar filter and back illuminated CMOS based 2d detector. The telescope designed for 6 U cubesat. The instrument itself has dimension of about 0.5 U with extended tube from 20 to 50 cm length.

Keywords: Pin-hole camera, solar corona, soft X-ray, cubesat.

DOI: 10.21883/TP.2022.08.54551.88-22

Introduction

Currently, there is a rapidly growing interest in conducting scientific and applied research on CubeSat-type spacecraft with a mass of several kilograms. Such platforms have a characteristic composite structure, which is formed from the simplest units 1 U with a size of approximately $10 \times 10 \times 10$ cm. This format was proposed more than 20 years ago and has not undergone significant changes since then [1]. The size of the satellites is growing at the same time. If at first CubeSats of the 1 U format were mainly launched, then already in 2020 nanosatellites of the 3 U format and more prevailed in launches. At the same time, the CubeSat market and their junctions is being commercialized, which makes it possible to assemble satellites from mass-produced components for the specific needs of scientific and applied experiments. CubeSats of the 6 U format have become widespread in the last 2–3 years, which allow you to place relatively large scientific equipment ($30 \times 10 \times 10$ cm and more), and are also usually equipped with a more accurate orientation and stabilization system, and in addition, allow the transmission of substantial amounts of scientific information to Earth.

Interest in CubeSats is also caused by the high cost and long preparation times for experiments on large spacecraft. This is especially important for studying and monitoring solar activity. Despite the huge scientific and applied interest in the results of solar observation, the number of new space solar observatories is very small. For this reason, there is a significant interest in the development of small-sized scientific instruments capable of working on nanosatellites

and CubeSats. This paper presents a project of a soft X-ray solar telescope based on a pinhole camera, which is adapted to work on a CubeSat.

1. Application of X-ray pinhole camera in solar astronomy

The issues of setting up experiments in the field of solar physics on CubeSats are being actively investigated. In particular, experiments have been carried out in recent years on photometry of X-ray solar radiation [2] and its spectral composition. Projects of the VUV telescopes of the [3] range are also being developed.

One of the most relevant areas of research of the Solar corona is the acquisition of images and spectra in the soft X-ray (SXR) region of the spectrum — 1–10 keV. Plasma ion lines in this range are excited at temperatures of several million degrees, which corresponds to flash processes. To the present time, grazing incidence telescopes [4] or imaging spectrometers based on Bragg crystal mirrors have been used to register solar images in the SXR range. Both types of instruments have significant dimensions due to the features of the optical system. Since the equipment being developed for nanosatellites is subject to serious restrictions on weight, dimensions, energy consumption and information content, traditional optical systems cannot be used. To obtain images in the SXR range on nanosatellites, it is proposed to use a pinhole camera, which is a small aperture in an opaque screen (Fig. 1).

The size of the pinhole image D is determined by the angular size of the image T and the distance from the

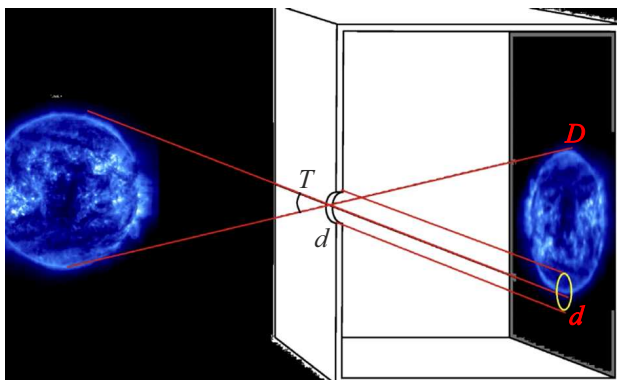


Figure 1. The principle of operation of the pinhole camera.

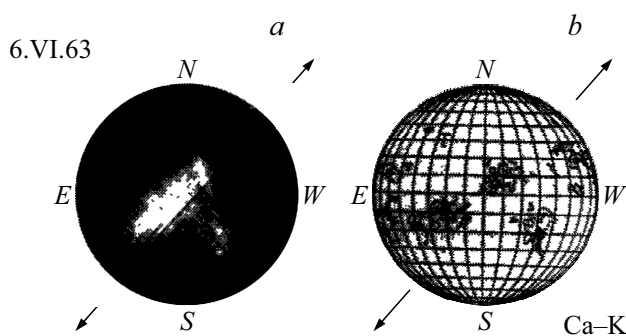


Figure 2. Image of the Sun obtained in the range 170–400 Å using a pinhole camera in FIAN in 1963 g. (a); obtained in the same period by a ground-based telescope in the line Ca–K (b).

aperture to the receiver plane, and the resolution, excluding diffraction, is determined by the aperture size d . Thus, the linear resolution in the receiver plane is determined by the ratio d/D .

Historically, the first experiments to register X-ray images in space were the American and Soviet experiments to observe the Sun in the early 60s of the last century [5,6]. Since there were no effective X-ray optics at that time, the images were constructed using a pinhole camera equipped with a thin-film filter to block visible radiation (Fig. 2). The disadvantages of this method of observation are the low aperture, the resolution determined by the ratio of the aperture diameter to the distance to the focal plane, as well as the polychromaticity of the recorded images, since the spectral range of such an instrument is determined primarily by the filter used. At the same time, the pinhole camera has a large field of view and ease of adjustment and operation. Currently, there are new projects of solar telescopes using pinhole cameras [7–9]. This is due to the development of two-coordinate silicon detectors, which make it possible to dramatically increase the information content of the instrument and obtain, in addition to spatial, spectral resolution.

Characteristics of the X-ray pinhole camera

Parameter	Value
Energy range, keV	1–20
Detector energy resolution, eV	60–150
Angular resolution, ″	40
Image size, cells	700 × 700
Image size, Kbyte	10
Exposure time at image acquisition, s	10–100
Minimum exposure time in spectroscopy mode, s	0.1

2. Brief description of the equipment

The image is formed in the plane of a two-coordinate silicon detector after the radiation passes through a hole in an opaque tungsten diaphragm with a thickness of 0.4 mm. To filter optical radiation, a thin-film filter made of aluminized mylar with a thickness of 10, μm is installed on the diaphragm.

To implement the tool, the following main characteristics of the pinhole camera were selected: aperture diameter 0.2 mm, distance from the aperture to the receiver plane 500 mm. This allows you to get the size of the image of the Sun on the detector with a size of approximately 5 mm. With the selected parameters, the resolution is about 40″. Image registration is carried out using a two-coordinate silicon detector. With small radiation fluxes (in the absence of powerful flashes and with a short exposure time), it is possible to isolate single photon events on the matrix and construct the corresponding spectrum.

The telescope will use an image receiver based on a back-side illuminated CMOS matrix of the Gpixel GSENSE2020BSI type with a format of 2048×2048 active pixels [10]. Pixel size is $6.5 \times 6.5 \mu\text{m}$. The dynamic range is 67.5 dB. The amplitude resolution when registering individual photons in the range 1 keV–60 eV.

The receiver has two modes of operation: image registration mode and individual photon counting mode. In the photon counting mode, an amplitude (spectral) analysis of the photon energy is possible. In image registration mode, pixels are binned (combined) in a square from 2×2 to 16×16 . Accordingly, the effective size of the image element ranges from 13×13 to $124 \times 124 \mu\text{m}$. To transmit information to the reset channel, software compression based on a discrete wavelet transform with subsequent arithmetic coding is implemented. The information compression ratio reaches 1:100, which makes it possible to obtain full-fledged images of the Sun with a size of no more than 10 Kbyte. The power consumption of the receiver is expected to be no more than 1.5 W in active and no more than 0.5 W in standby mode. The communication interface with the satellite's onboard systems will be carried out via

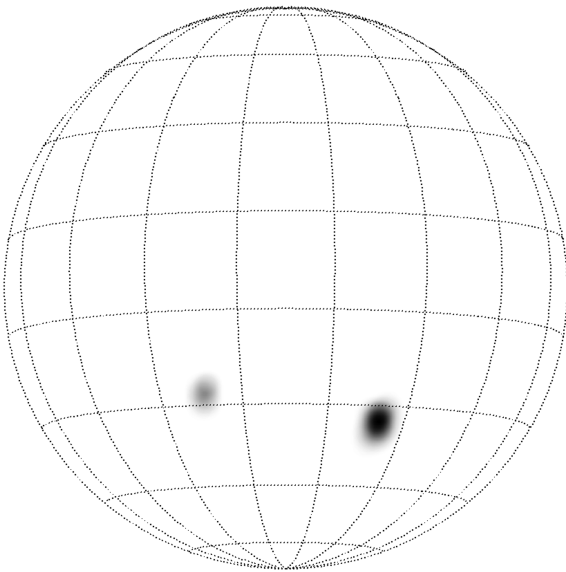


Figure 3. Model image of the Sun according to the X-ray pinhole camera.

RS485 or CAN interfaces. The characteristics of the tool are listed in the following table.

Fig. 3 shows a model image of the Sun in the SXR range in the form in which it would be registered by the developed pinhole camera. In general, the spatial resolution of the pinhole camera is worse than that of devices with more complex optical circuits, which, however, is not critical, since the study of the structure of radiation sources is not included in the list of priority tasks of the device. Also, it can be noticed that the image according to the pinhole camera is inverted relative to the original, which is a feature of the principle of constructing the image itself.

Conflict of interest

The authors declare that they have no conflict of interest.

References

- [1] *CDS. CubeSat Design Specification. Rev. 13* (California Polytechnic State University, 2015), 42 p.
- [2] J.P. Mason, T.N. Woods, A. Caspi, P.C. Chamberlin, C. Moore, A. Jones, R. Kohnert, X. Li, S. Palo, S.C. Solomon. *J. Spacecraft Rockets*, **53** (2), 328–339 (2016). DOI: 10.2514/1.A33351
- [3] S.V. Kuzin, S.A. Bogachev, N.F. Erkhova, A.A. Pertsov, I.P. Loboda, A.A. Reva, A.A. Kholodilov, A.S. Ulyanov, A.S. Kirichenko, I.V. Malyshev, A.E. Pestov, V.N. Polkovnikov, M.N. Toropov, N.N. Tsybin, N.I. Chkhalo, V.A. Kryukovsky, V.N. Gorev, A.A. Doroshkin, A.M. Zadorozhny, V.Yu. Prokopyev. *ZhTF*, **91** (10), 1441 (2021) (in Russian). DOI: 10.21883/JTF.2021.10.51355.115-21
- [4] S. Tsuneta, L. Acton, M. Bruner, J. Lemen, W. Brown, R. Carvalho, R. Catura, S. Freeland, B. Jurcevich, M. Morrison, Y. Ogawara, T. Hirayama, J. Owens. *Sol. Phys.*, **136** (1), 37 (1991). DOI: 10.1007/BF00151694

- [5] R.L. Blake, T.A. Chubb, H. Friedman, A.E. Unzicker. *Astrophys. J.*, **137**, 3 (1963). DOI: 10.1086/147479
- [6] S.L. Mandelstam. *Space Sci. Rev.*, **4**, 587 (1965). DOI: 10.1007/BF00216272
- [7] J. Sylwester, S. Płoceniak, J. Bakała, Ż. Szaforz, M. Stęślicki, D. Ścisłowski, M. Kowaliński, P. Podgórski, J. Hernandez, S. Shestov. *Proc. Int. Astron. Union*, **305**, 114 (2015). DOI: 10.1017/S1743921315004627
- [8] A. Caspi, A.Y. Shih, H. Warren, A.R. Winebarger, T.N. Woods, C.M.M. Cheung, C. DeForest, J.A. Klimchuk, G.T. Laurent, J.P. Mason, S.E. Palo, R. Schwartz, D.B. Seaton, M. Steslicki, S. Gburek, J. Sylwester, T. Mrozek, M. Kowaliński, M. Schattenburg. *American Geophysical Union* (2020) #SH048-0007.
- [9] A. Kirichenko, S. Kuzin, S. Shestov, A. Ulyanov, A. Pertsov, S. Bogachev, A. Reva, I. Loboda, E. Vishnyakov, S. Dyatkov, N. Erkhova, M. Stęślicki, J. Sylwester, S. Płoceniak, P. Podgórski, M. Kowaliński, J. Bakała, Ż. Szaforz, M. Siarkowski, D. Ścisłowski, T. Mrozek, B. Sylwester, I. Malyshev, A. Pestov, V. Polkovnikov, M. Toropov, N. Salashchenko, N. Tsybin, N. Chkhalo. *Front. Astron. Space Sci.*, **8**, 66 (2021). DOI: 10.3389/fspas.2021.646895
- [10] *Gpixel products* [Electronic resource] Available at: <https://www.gpixel.com/products/area-scan-en/gse-nse/gsense2020bsi>